Theoretical Study of the Hydrogen Release from Ammonia Alane and the Catalytic Effect of Alane

ARTICLE *in* THE JOURNAL OF PHYSICAL CHEMISTRY C · APRIL 2008

Impact Factor: 4.77 · DOI: 10.1021/jp7103374

7 AUTHORS, INCLUDING:

Nguyen Vinh Son
University of Leuven
35 PUBLICATIONS **488** CITATIONS
SEE PROFILE

Minh Tho Nguyen
University of Leuven
748 PUBLICATIONS **10,835** CITATIONS
SEE PROFILE

Vu Thi Ngan
Quy Nhon University
32 PUBLICATIONS **558** CITATIONS
SEE PROFILE

David A Dixon
University of Alabama
766 PUBLICATIONS **22,167** CITATIONS
SEE PROFILE

Theoretical Study of the Hydrogen Release from Ammonia Alane and the Catalytic Effect of Alane

Vinh Son Nguyen,[#] Myrna H. Matus,[§] Vu Thi Ngan,[#] Minh Tho Nguyen,*[,#,§] and David A. Dixon*[,§,†]

Department of Chemistry, The University of Alabama, Shelby Hall, Tuscaloosa, Alabama 35487-0336, and Department of Chemistry, University of Leuven, B-3001 Leuven, Belgium

Received: October 25, 2007; In Final Form: December 19, 2007

Electronic structure calculations at the CCSD(T) level with the aug-cc-pVnZ and aug-cc-pV(n+d)Z basis sets (n = D, T, and Q) were employed to construct the potential energy surfaces for H_2 release from ammonia alane without and with the presence of alane (AlH_3). In the AlH_3NH_3 monomer, although the energy barrier for H_2 loss of ∼29 kcal/mol is comparable with the energy for Al−N bond cleavage (∼27 kcal/mol), kinetics calculations show that only the latter is important at 298 K. The calculated results demonstrate that alane can play the role of an efficient bifunctional catalyst for H_2 release from ammonia alane. The transition state for H_2 production from AlH_3NH_3 + AlH_3 is located 4.3 kcal/mol lower in energy than the separated reactants and 18.7 kcal/mol above the complex AlH_3NH_3···AlH_3. A systematic comparison with the reaction pathways for H_2 loss from ammonia borane (BH_3NH_3) with AlH_3 or BH_3 as the catalyst shows that alane is a better catalyst than borane. The predicted kinetic rate constants for hydrogen elimination from ammonia alane with alane as the catalyst are $k(298\ K) = 2.6 \times 10^{-2}\ s^{-1}$ and $k(400\ K) = 8.4 \times 10^{1}\ s^{-1}$, including tunneling corrections.

Introduction

There is considerable interest in the development of hydrogen-based fuel cells for use as environment-friendly alternatives to fossil oil in the transportation sector.[1] Hydrogen storage is one of the critical issues that must be addressed for hydrogen to be a practical fuel for this use. Extensive efforts are underway to design and synthesize materials for efficient chemical H_2 storage. With a low molecular weight (30.9 g mol^{-1}) and a high potential H_2 capacity (19.6 wt %), in conjunction with both acidic NH and basic BH bonds, ammonia borane (BH_3NH_3, **ab**) and its derivatives are currently being considered as a hydrogen source.[2] We have previously shown that molecular **ab** and the corresponding salt [BH_4^-][NH_4^+] could serve as good hydrogen storage systems that release H_2 in slightly exothermic processes.[3] Due to the fact that the energy barrier for thermal H_2 elimination from the **ab** monomer, ∼36 kcal/mol,[4] is higher than the B−N bond energy, an efficient catalyst will be required for the release of H_2 at temperatures appropriate for use with fuel cells. Recent experimental studies have considered the acid-catalyzed,[5] and base-transition-metal-catalyzed[6] dehydrogenation processes, and enhanced dehydrogenation from **ab** has also been observed in ionic liquids.[7]

By using ab initio quantum chemical calculations, we recently demonstrated that the Lewis acid borane (BH_3) can act as a bifunctional acid−base catalyst, greatly accelerating the H_2 formation from **ab**.[4] With BH_3 as a catalyst, the energy barrier for H_2 release is reduced from 36 to 6 kcal mol^{-1} with respect to the asymptotic reactants. BH_3 was also found to induce a similar catalytic effect on H_2 formation from diphosphine (P_2H_4).[8] Ammonia also acts as a Lewis base catalyst for H_2 release from **ab**, but the resulting energy barrier is higher than that for BH_3.[4]

Whereas the neutral dimer of **ab** ((BH_3NH_3)$_2$) was shown to play a minor role in the release of H_2 from ammonia borane, the isomeric ion pairs [$BH_3NH_2BH_3^-$][NH_4^+] and [$NH_3BH_2NH_3^+$]-[BH_4^-] play an important role,[9] consistent with experimental observations, in ionic liquids and the solid state.[10] Ammonium salts of boron hydride anions and dianions may also serve as good materials for H_2 production.[11] We have confirmed that a catalyst is needed to develop adequate reaction conditions for the H_2 release from ammonia triborane ($B_3H_7NH_3$).[12,13]

Metal-doped alanes such as $NaAlH_4$ have long been considered as hydrogen storage media.[14] Recent experimental studies have suggested that alane (AlH_3), the heavier analogue of borane, could also be a promising material for onboard hydrogen storage applications,[15] consistent with earlier predictions.[19] Reactions of aluminum hydride derivatives with **ab** generate AlN/BN materials upon thermal dehydrogenation at high temperatures.[16] The complex of alane with the organic amine triethylenediamine (TEDA) was first synthesized by Ashby with a pressure of H_2 of 340 bar.[17] Recently, Graetz at al. reported a new synthetic approach to this complex at a pressure of H_2 less than 30 bar.[18] By using high-accuracy ab initio electronic structure theory to calculate the heats of formation and reaction thermodynamic parameters, both in the gas phase and solid state, we predicted that molecular ammonia alane (AlH_3NH_3, **aal**) and the corresponding ionic salt [AlH_4^-][NH_4^+] in the solid state can serve as good hydrogen storage systems that release H_2 in near-thermoneutral processes.[19] The isovalent phosphorus systems including borane phosphine (BH_3PH_3) and phosphine alane (AlH_3PH_3), and their corresponding crystal salts [XH_4^-][PH_4^+], with X = B and Al, have also been predicted to have appropriate thermodynamic properties to serve as H_2 storage systems.

* To whom correspondence should be addressed.
† E-mail: dadixon@as.ua.edu.
§ The University of Alabama.
# University of Leuven.

10.1021/jp7103374 CCC: $40.75
Published on Web 03/18/2008

The potential of a compound for chemical hydrogen storage is dependent not only on the percent of H_2 stored by weight but also on the inherent kinetics and mechanism of the processes releasing H_2 and regenerating the compound which stores H_2. We use high-level molecular orbital theory to predict the molecular mechanism of H_2 release from **aal** and the ability of alane to serve as a catalyst for hydrogen release on the basis of the following reactions

$$AlH_3NH_3 \rightarrow H_2 + AlH_2NH_2 \quad (1)$$

$$AlH_3NH_3 + AlH_3 \rightarrow H_2 + AlH_3 + AlH_2NH_2 \quad (2)$$

$$BH_3NH_3 + AlH_3 \rightarrow H_2 + AlH_3 + BH_2NH_2 \quad (3)$$

$$AlH_3NH_3 + BH_3 \rightarrow H_2 + BH_3 + AlH_2NH_2 \quad (4)$$

For comparison purposes, H_2 loss from ethane catalyzed by AlH_3 was also considered.

Computational Methods

The molecular orbital theory calculations were carried out by using the Gaussian 03[20] and Molpro 2006[21] suites of programs. We used the augmented correlation-consistent (aug-cc-pVnZ) basis sets.[22] For the sake of brevity, we abbreviate the basis sets to aVnZ, with n = D, T, and Q. In the first series of calculations for all structures, geometries and vibrational frequencies were initially determined using the second-order perturbation theory MP2[23] with the correlation-consistent aVDZ basis set. Geometries of the important equilibrium and transition-state (TS) structures were refined using the same correlation treatment with the larger aVTZ basis set at the MP2 level. Relative energies were then calculated at the coupled-cluster theory CCSD(T)[24,25] level at the MP2/aVTZ geometries with both the aVDZ and aVTZ basis sets. MP2/aVDZ frequency calculations were also carried out, where the results were scaled by 0.97, as described in previous studies.[3,19a]

In addition to the above set of calculations, we also studied the AlH_3NH_3 systems and selected stationary points of the ($AlH_3NH_3BH_3$) supersystem at a higher level. It has been established that tight d functions are necessary for calculating accurate atomization energies for second-row elements.[19,26] Therefore, we also included a set of tight d functions for Al in our calculations. Basis sets containing additional tight d functions are denoted as aug-cc-pV(n+d)Z or as aV(n+d)Z. For the reaction pathways of **aal**, geometry parameters were reoptimized using the aV(T+d)Z basis set. Two different series of CCSD(T) single-point electronic energy calculations were carried out (i) by first using the aVnZ basis sets, with n = D, T, and Q, based on MP2/aVTZ geometries, and (ii) with the second series using the aV(n+d)Z basis set, based on MP2/aV(T+d)Z geometries. The final total valence electronic energies were then extrapolated to the complete basis set (CBS) limit at the CCSD(T) level using the following expression[27]

$$E(n) = A_{CBS} + B \exp[-(n-1)] + C \exp[-(n-1)^2] \quad (5)$$

with $n = 2$, 3, and 4 for the aVnZ and aV(n+d)Z, n = D, T, and Q, basis sets, respectively.

The kinetics for H_2 elimination was studied with transition-state theory (TST)[28,29] using the KHIMERA program,[30] where the thermal rate constant in the thermodynamic formulation is given by eq 6[28]

$$k_\infty(\mathrm{TST}) = \frac{k_B T}{h} \exp\frac{\Delta S^\ddagger}{R} \exp\frac{-\Delta H^\ddagger}{RT} \quad (6)$$

and the high-pressure limit pre-exponential factor is given by $A = (k_B T/h)\cdot\exp(\Delta S^\ddagger/R)$. Note that the E_a of the Arrhenius expression from TST and $\Delta H^\ddagger$ are related by $E_a = \Delta H^\ddagger + RT$ for a unimolecular process. We also used RRKM theory[31] to predict the rate constants using the following expression

$$k_{uni} = \frac{\sigma}{h}\left[\frac{N^\ddagger(E - E_0)}{\rho(E)}\right] \quad (7)$$

where σ is the symmetry number. Evaluation of the sum ($N^\ddagger$) and density (ρ) of states was carried out by KHIMERA. We applied N_2 as the bath gas in the temperature range (T) from 200 to 2000 K and pressure range (p) from 0.1 to 8360 Torr. The tunneling corrections were calculated using the Skodje and Truhlar (ST)[32] equations, which include the imaginary frequency, the energy barrier, the reaction energy, $\Delta H^\ddagger$, the zero-point-corrected barrier height, and ΔH_R, the reaction exothermicity, both at 0 K

$$Q_{tunnel,ST}(T) = \frac{\beta\pi/\alpha}{\sin(\beta\pi/\alpha)} - \frac{\beta}{\alpha - \beta}\exp[(\beta - \alpha)(\Delta H^\ddagger - \Delta H_R)] \quad (8a)$$

this expression is valid for $\alpha \geq \beta$. In the case where $\beta \geq \alpha$

$$Q_{tunnel,ST}(T) = \frac{\beta}{\beta - \alpha}\{\exp[(\beta - \alpha)(\Delta H^\ddagger - \Delta H_R)] - 1\} \quad (8b)$$

with $\beta = 1/k_B T$ and $\alpha = 2\pi/h\omega_i$, where ω_i is the imaginary frequency at the transition state; when the reaction is exoergic, ΔH_R is equal to zero.

Results and Discussion

Tables S1 and S2 of the electronic Supporting Information (ESI) list the total and zero-point energies calculated at different levels of theory. Table S3 lists the coordinates of all MP2/aVTZ-optimized geometries. Figure S1 of the ESI displays selected optimized geometries of the structures that are not included in the text.

Hydrogen Release from Ammonia Alane. The results obtained for the unimolecular fragmentation of AlH_3NH_3 are summarized in Figure 1. Geometries and energetics of both the reactant and product have been analyzed in detail.[19] The reaction is of nearly thermoneutral character, with a small reaction enthalpy of about ~3 kcal/mol.

The variations of the MP2 parameters are very small following the addition of tight d-polarization functions to the Al basis set, with the distances changing by ~0.006 Å. The shape of the **aal-ts** is similar to that of the TS for H_2 elimination from the lower homologue ammonia borane.[4] The **aal-ts** has C_s point group symmetry, and formation of the H−H bond occurs within the molecular plane. Both N−H and Al−H bonds are broken, but the N−H is proportionally more stretched. Initiated by rotation about the Al−N bond, both migrating H atoms are displaced in opposite directions toward each other, parallel to the Al−N bond. The H(N) atom is moving farther toward the Al, in such a way that both departing H atoms are equidistant with respect to the Al center. The H−H distance of 1.01 Å is nearly the same as that of 0.99 Å in the TS of BH_3-NH_3 reported previously (MP2/aVTZ values).[4] The **aal-ts** has the geometry of a slightly cis-distorted amino alane interacting

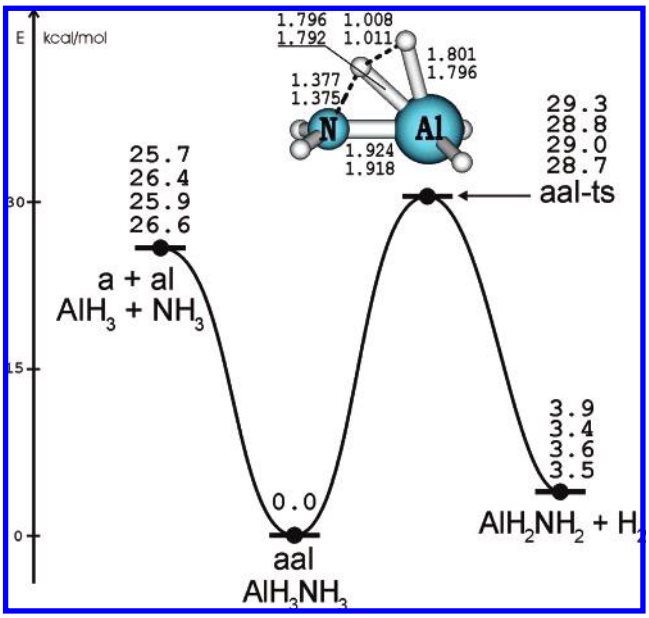

Figure 1. Schematic minimum-energy pathways for H_2 release and Al−N bond dissociation from **aal**. Relative energies in kcal/mol from calculations at the levels: upper, CCSD(T)/aVTZ; middle upper, CCSD(T)/CBS-aVnZ; middle lower, CCSD(T)/aV(T+d)Z; and lower, CCSD(T)/CBS-aV(n+d)Z. All values are corrected for zero-point contributions. Selected geometry parameters of the transition state for H_2 release, **aal-ts**, using the MP2 method with two basis sets: upper, aug-cc-pVTZ and lower, aug-cc-pV(T+d)Z. Bond distances are in angstroms, and bond angles are in degrees.

with an elongated H_2 at N and Al. The elongated H_2 is a dominant feature and accounts for a large part of the resulting energy barrier.

As for BH_3NH_3, **aal** decomposition is characterized by two different channels, Al−N bond cleavage and H_2 loss. The results calculated using four different levels as shown in Figure 1 are consistent and show relatively small effects of the additional tight d functions on the relative energies. The two sets of CCSD(T) results using the two CBS energies based on one-electron basis sets without and with tight d functions differ from each other by at most 0.3 kcal/mol. The larger basis set tends to reduce, marginally but systematically, the relative energies. Our best estimate using CCSD(T)/CBS-aV(n+d)Z electronic energies places the fragments AlH_3 + NH_3 and the TS **aal-ts** 26.6 and 28.7 kcal/mol above **aal**, respectively. Although the bond dissociation remains favored energetically, the difference in these energies is small, 2.1 kcal/mol, as compared to the difference of 10.4 kcal/mol in BH_3NH_3 favoring B−N bond dissociation (B−N bond energy = 26.0 kcal/mol).[4] Whereas the energies of the N−X bonds (X = B, Al) are almost equal, the energy barrier is substantially reduced upon going to the heavier element. Due to the larger difference in electronegativity, the Al−N and Al−H bonds are more polar than the B−N and B−H bonds, in particular the $Al^{\delta+}-H^{\delta-}$ bond. The H(Al) atom is more negatively charged (∼−0.4 e) than H(B), and this hydride can capture more easily the incipient proton $H(N)^+$ to form the $H^{\delta+}-H^{\delta-}$ bond.

The effect of different basis sets in predicting the relative energies is also shown in Table 1. The values obtained using the aVTZ basis set differ by ∼0.2 kcal/mol from those evaluated with the larger aV(T+d)Z basis set. This is consistent with the small geometry changes noted above upon extension of basis functions. If we use the CCSD(T)/CBS-aV(n+d)Z results as the reference values, the CCSD(T)/aVTZ values differ by similar amounts, 0.9 kcal/mol for the dissociation energy and −0.6 kcal/mol for the barrier height. Such differences are consistent with the results recently obtained for a large set of boron−nitrogen compounds[9,12] and show that we can employ the CCSD(T)/aVTZ + ZPE level of theory to construct the potential energy surfaces of the larger systems to within ±1.0 kcal/mol as compared to the best theoretical estimates.

TABLE 1: Relative Energies (kcal/mol) of the Equilibrium Structures in the Process of H_2 Elimination from AlH_3NH_3 at the CCSD(T) Level

structures	aVTZ[a]	CBS[a]	aV(T+d)Z[b]	CBS[b]
$AlH_3 + NH_3$	25.7	26.4	25.9	26.6
AlH_3NH_3 (**aal**)	0.0	0.0	0.0	0.0
aal-ts	29.3	28.8	29.0	28.7
$AlH_2NH_2 + H_2$	3.9	3.4	3.6	3.5

[a] MP2/aVTZ-optimized geometries. [b] MP2/aV(T+D)Z-optimized geometries.

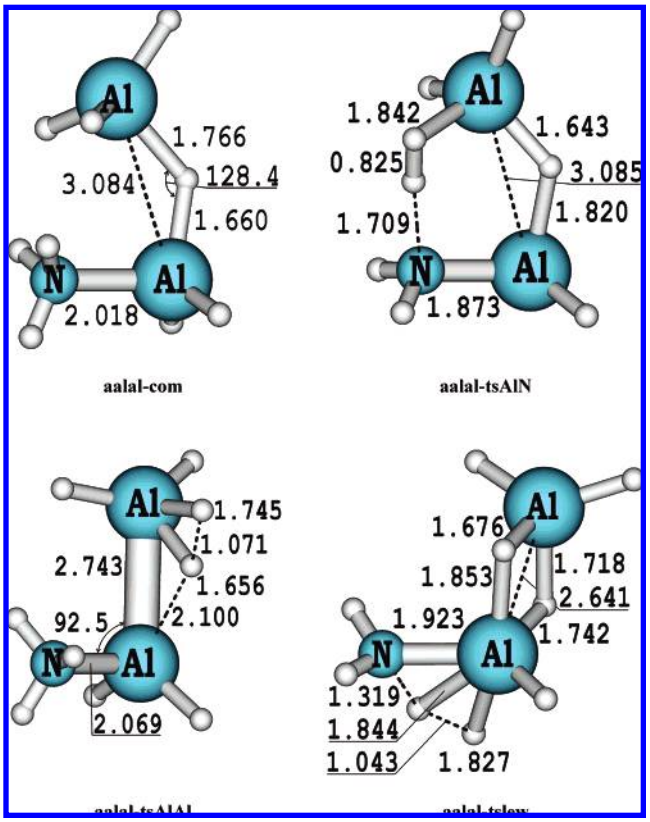

Figure 2. Selected MP2/aVTZ geometry parameters of an adduct and three transition states related to the reaction AlH_3NH_3 + AlH_3 (**aal** + **al**). Bond distances are in angstroms, and bond angles are in degrees.

Hydrogen Release from Ammonia Alane with Alane as a Catalyst. Even though H_2 release from the **aal** monomer has a lower barrier than that found for BH_3NH_3, an energy barrier of ∼29 kcal/mol is still too high to be practical, and the process will be competing with Al−N bond dissociation. The latter is favored not only by the smaller activation enthalpy but also by a larger activation entropy (larger frequency factors) and hence larger rate constants.[12] In our previous studies on H_2 elimination from BH_3NH_3 [4] and P_2H_4,[8] we showed that a BH_3 molecule could act as a Lewis acid catalyst for H_2 release from these materials. We now consider whether an AlH_3 molecule, **al**, produced from the bond cleavage channel of **aal** can serve as a catalyst. The MP2/aVTZ-optimized geometries are summarized in Figure 2 for selected geometries, and the schematic potential energy profiles are shown in Figure 3. Table 2 lists the relative energies calculated at different levels of theory for H_2 release from ammonia alane with alane as a catalyst.

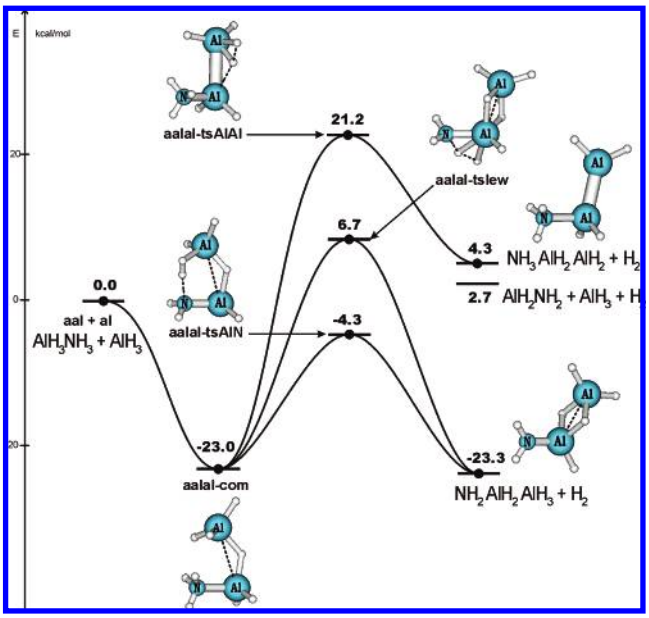

Figure 3. Schematic energy profiles illustrating three different reaction pathways for H_2 release from **aalal-com**. Relative energies in kcal/mol are from CCSD(T)/aVTZ + ZPE calculations.

TABLE 2: Relative Energy (kcal/mol) of the Reactants, Complexes, Transition States, and Products in the Processes of H_2 Elimination from AlH_3NH_3 in the Presence of AlH_3

molecule	MP2/ aVTZ	CCSD(T)/ aVDZ	CCSD(T)/ aVTZ
$AlH_3NH_3 + AlH_3$	0.0	0.0	0.0
$AlH_2NH_2 + AlH_3 + H_2$	3.9	4.3	2.7
$NH_2AlH_2AlH_3 + H_2$	−24.8	−16.8	−23.3
$NH_3AlH_2AlH_2 + H_2$	2.6	7.3	4.3
aalal-com	−23.0	−21.1	−23.0
aalal-tsAlAl	22.6	23.3	21.2
aalal-tsAlN	−5.9	−1.0	−4.6
aalal-tslew	5.4	11.3	6.7

The initial barrier-free interaction of **aal** and **al** gives rise to the adduct **aalal-com**, 23.0 kcal/mol *below* the separated reactants **aal** + **al**. The adduct is characterized by a single Al−H−Al bridge and an Al−N bond, and in many aspects, its shape is similar to the condensation adduct between BH_3NH_3 and BH_3.[4] Starting from **aalal-com**, three TS's have been located, each representing a different type of hydrogen elimination.

Transition-state **aalal-tsAlAl** is 21.2 kcal/mol above **aal** + **al** and is the highest-lying TS. Ammonia acts as a conventional Lewis base interacting with a rearranging dialane from which H_2 is formed. A H from the central Al is transferred so that the departing H_2 with a H−H distance of 1.071 Å is located closer to the terminal Al. The high-energy barrier of 44.2 kcal/mol, with respect to **aalal-com**, can be accounted for by disfavored charge distributions as both departing H atoms are negative. The product $NH_3AlH_2AlH_2$ is a complex of ammonia with Al_2H_4 and is 4.3 and 27.3 kcal/mol above the reactants and adduct, respectively.

The second TS **aalal-tslew** consists of a Lewis acid interaction between **al** and the monomer TS **aal-ts** described above. Compared with **aal-ts**, the longer Al−H and H−H and shorter N−H distances in **aalal-tslew** are indicative of an earlier TS. The two AlH_3 groups constitute a double Al−H−Al bridge bond as in dialane, and this typical bonding mode leads to an energetic lowering. The **aalal-tslew** is 6.7 and 29.7 kcal/mol above the reactants and adduct, respectively. The product from this TS is aminodialane $NH_2AlH_2AlH_3$, which conserves the dialane double bridge form and is 23.3 kcal/mol below the reactants and 0.3 kcal/mol below the adduct **aalal-com**. $NH_2AlH_2AlH_3$ dissociates to products $NH_2AlH_2 + AlH_3$ with a dissociation energy of 26.0 kcal/mol.

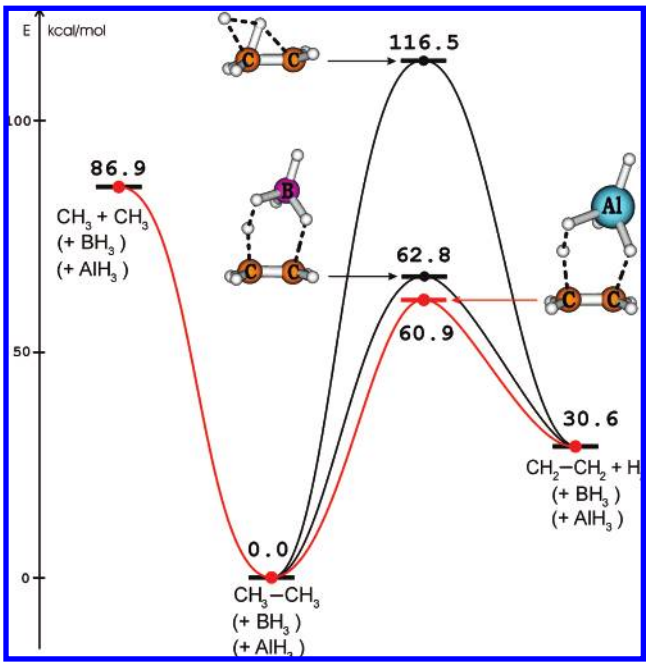

Figure 4. Schematic energy profiles showing the pathways for H_2 release from ethane, ethane + borane, and ethane + alane. Relative energies in kcal/mol are from CCSD(T)/aVTZ + ZPE calculations.

The third TS structure **aalal-tsAlN** is a member of the class of six-member cyclic TS's previously found for the analogous $BH_3NH_3 + BH_3$ system, in which BH_3 exerts a beneficial catalytic effect.[4] Relative to the adduct **aalal-com** geometry, the Al−H−Al bridge in the TS remains intact, and the H−H bond is formed within the N−H−H−Al skeleton. The H−H distance of 0.825 Å is even shorter than that in the corresponding TS of the $BH_3NH_3BH_3$ supersystem and indicates that H_2 formation is basically complete. This TS looks like a structure in which a H_2 molecule is encapsulated by an aminodialane molecule through a dihydrogen bond. In fact, this channel leads to the same product as **aalal-tslew**, aminodialane plus molecular hydrogen. Similar to the monomer case, the higher polarity within the $Al^{\delta+}-H^{\delta-}-H^{\delta+}-N^{\delta-}$ framework tends to lower the barrier for H-atom transfers. Such stabilization is clearly found in the low-lying energy of **aalal-tsAlN**, which is 4.3 kcal/mol below **aal** + **al** and 18.7 kcal/mol above **aalal-com**.

Of the three channels identified for the H_2 release from **aal** in the presence of **al**, the channel involving a six-member cyclic TS **aalal-tsAlN** exhibits a substantial reduction in the energy barrier. This result clearly demonstrates a catalytic action of alane taking place via an active participation in a bifunctional hydrogen atom transfer.

Hydrogen Release from Ethane with Alane as a Catalyst. Having established that alane is an improved catalyst for H_2 production from AlH_3NH_3, we also examined whether it can reduce the barrier to loss of H_2 in ethane as did BH_3. Loss of H_2 from C_2H_6 to generate C_2H_4 is a Woodward−Hoffmann-forbidden reaction with an energy barrier of 116.5 kcal/mol, higher than the C−C and C−H bond energies of 86.9 and 100.8 kcal/mol, respectively. We previously showed[4] that BH_3 can catalyze this reaction. Figure 4 shows the energy profile of the reaction. The shape of the TS **tset-al** is similar to that involving borane (**tset-b** reported in ref 4), or **aalal-tsAlN** described above, with the reacting atoms assembling in a six-member ring for

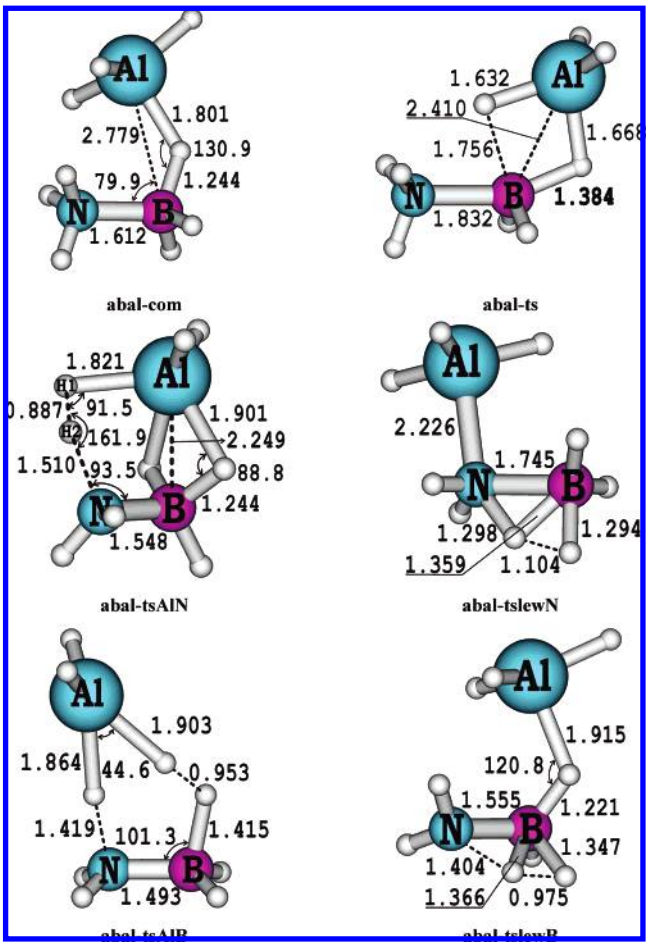

Figure 5. Selected MP2/aVTZ geometry parameters of the adduct, transition structures, and products related to H_2 elimination of BH_3-NH_3 + AlH_3. Bond distances are in angstroms, and bond angles are in degrees.

hydrogen transfer. The energy profiles show that alane is a slightly better catalyst than borane, reducing the barrier height by an additional ~2 kcal/mol. Although the energy barrier remains high, the BH_3 or AlH_3 decrease the barrier by >50 kcal/mol.

Hydrogen Release from Ammonia Borane with Alane as a Catalyst. We have studied the release of H_2 from **ab** with **al** as a catalyst. Figures 5 and 6 display the calculated geometries and energies, respectively, for the reaction pathways for **ab** + **al**. The approach of **al** to **ab** leads to a strong adduct **abal-com** characterized by a B−H−Al bridge. The bridged Al−H distance of 1.801 Å is markedly longer than that of 1.580 Å in AlH_3 or that of 1.752 Å in the mixed dimer BH_3AlH_3. The **abal-com** is 18.9 kcal/mol more stable than the isolated **ab** + **al** systems, similar to the value of 17.8 kcal/mol predicted for the complex between **ab** and **b**.[4] Four TS's for H_2 release have been found, **abal-tsAlB**, **abal-tslewB**, **abal-tslewN**, and **abal-tsAlN** (Figure 5). As discussed above, the letters **lew** refer to a Lewis type of interaction of either NH_3 or BH_3.

In **abal-tsAlB**, the departing H_2 molecule is formed within a B−H−H−Al bond. Because both H atoms are negatively charged, the repulsion results in a substantial energy barrier of 62.8 kcal/mol relative to the adduct (43.9 kcal/mol above reactants). Intrinsic reaction coordinate (IRC) calculations show formation of the fragmented products, H_2 + BH_2NH_2 + AlH_3, −6.4 kcal/mol below the reactants.

The **abal-tslewB** corresponds to a Lewis-type TS with the **al** interacting with a $H^{\delta-}$(B) giving rise to an Al−H−B bridge. The H_2 is lost from the B as a H(N) is transferred to the B. This transition state is similar to **abal-ts**, except that there is no interaction of a H(Al) with the B. The energy barrier via this TS is lower, 46.5 and 27.6 kcal/mol with respect to the adduct and reactants, respectively. The same separated products as those above have been generated.

The **abal-tslewN** is a Lewis-type TS with the **al** interacting with the lone pair on nitrogen. A H(N) is transferred to the B, and this structure is only slightly stabilized with respect to **abal-tslewB**. The **abal-tslewN** is 44.2 and 25.3 kcal/mol above the adduct and reactants, respectively. The three-member ring with an Al−H−B bridge is found to be the most stable product, and with the product H_2, this asymptote is 36.0 kcal/mol below the reactants.

The energetically most favorable TS is **abal-tsAlN**, which contains an Al−H−H−N skeleton as well as two Al−H−B bridge bonds. The H1−H2 distance of 0.887 Å shows that the departing H_2 is virtually formed at the transition state. The atomic charges recorded in Figure 7 show that the N atom is negatively charged (q_N = −1.01 electron) and that the Al is positively charged (q_{Al} = 1.21 electron). Together with a negative charge on H1 and a positive charge on H2, the $Al^{\delta+}$−$H1^{\delta-}$−$H2^{\delta+}$−$N^{\delta-}$ group constitutes a dihydrogen bond, similar to the B−H−H−N bond which strongly stabilizes the **ab** oligomers.[12] Another feature of **abal-tsAlN** is that when H1 of AlH_3 is transferred to H2 of NH_3, a H atom of BH_3 is transferred to Al to form the second B−H−Al bridge bond. This region of the TS is similar to that in BH_3AlH_3. Two B−H−B bridge bonds are not found in the **ab** + **b** system. The combination of these effects stabilizes **abal-tsAlN**, which is 20.6 kcal/mol above the adduct and only 1.7 kcal/mol above the separated reactants. The resulting product $NH_2BH_2AlH_3$ + H_2 asymptote is 15.0 kcal/mol below the reactants and 3.9 kcal/mol above the initial adduct. From **abal-com**, another channel can open on the potential energy surface, leading to the region of the AlH_3BH_3 + NH_3 reaction, which is 12.0 kcal/mol more stable than **ab** + **al**. The corresponding TS **abal-ts** is 17.8 kcal/mol above the reactants, suggesting that this channel is not competitive with the channel going through **abal-tsAlN**.

Figure 7 displays the topology of **abal-tsAlN** established using the atoms-in-molecules (AIM) approach.[33] As suggested by the short distance, formation of the H_2 molecule is well advanced. There exists a bond critical point (BCP) between H1 and H2, with a bond index of 0.58. BCP's are also located between Al and $(H)_2$ and B and $(H)_2$, even though the bond index of Al−$(H)_2$ (0.13) is much smaller than that of B−$(H)_2$ (0.79). These results together with a ring critical point (RCP) within the Al−H−H−B frame are consistent with the formation of the two bridge Al−H−B bonds. Another RCP is located within the Al−H−B−N−H2−H1 frame, suggesting the presence of cyclic electronic reorganization within this frame. From an electronic point of view, the catalytic action of alane is quite similar to that of borane[4] and accentuates the catalytic effect due to its higher polarity.

Hydrogen Release from Ammonia Alane with Borane as a Catalyst. Besides the channels shown in Figure 6, the (AlH_3-BH_3NH_3) potential energy surface has another channel with AlH_3NH_3 + BH_3 as a reactant asymptote, which is 0.2 kcal/mol lower in energy than BH_3NH_3 + AlH_3. This channel is also relevant to H_2 production in that decomposition of **aal** is now assisted by **b**. The geometries for this set of reaction paths are given in Figure 8, and the energy profiles are given in Figure 9. The main difference between the two initial adducts formed from condensation of NH_3 with AlH_3BH_3 is that the original

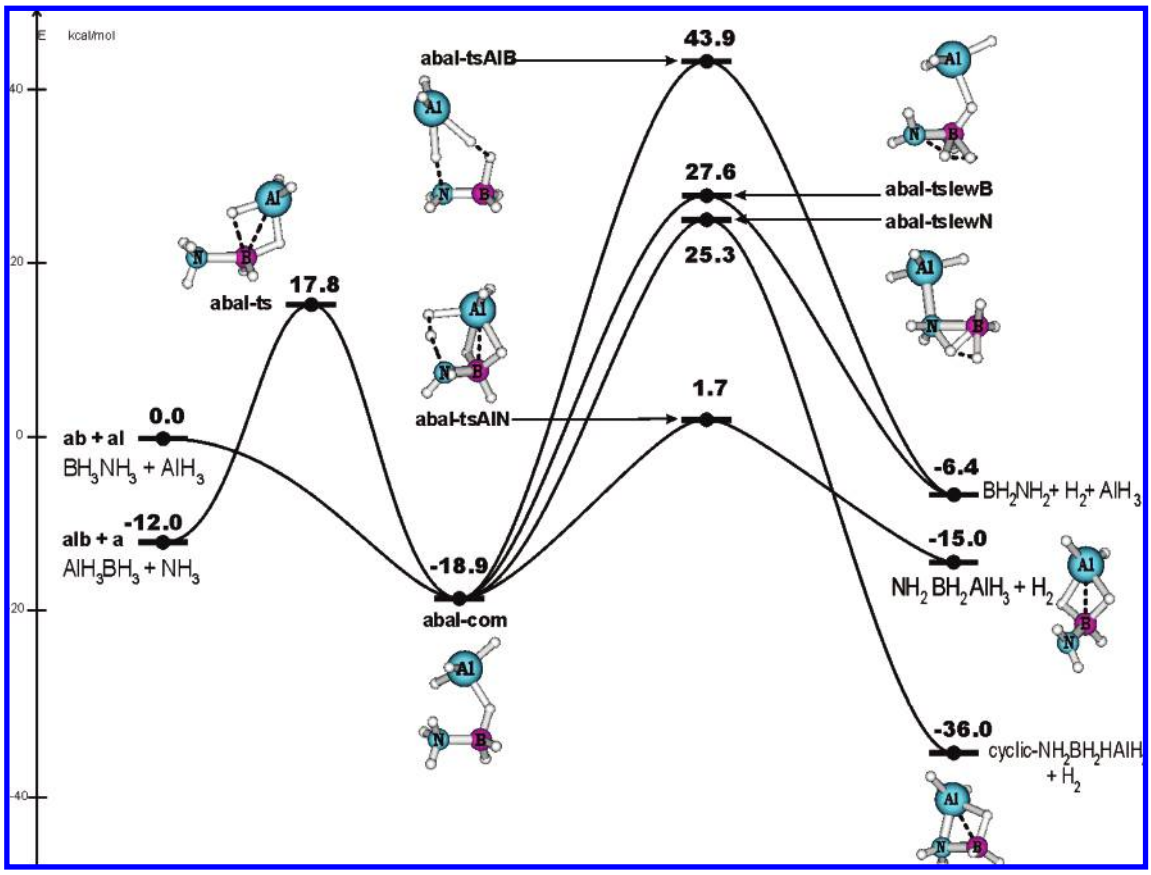

Figure 6. Schematic reaction pathways for H_2 release from $BH_3NH_3 + AlH_3$ and $AlH_3BH_3 + NH_3$ Relative energies in kcal/mol are from CCSD-(T)/aVTZ + ZPE calculations.

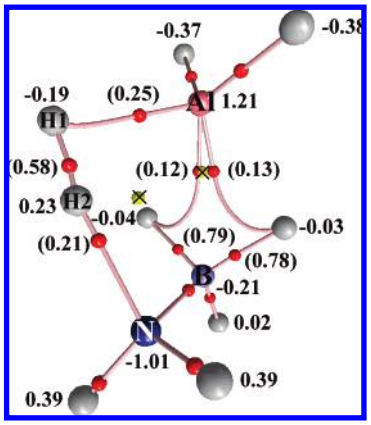

Figure 7. Molecular graph of **abal-tsAlN**. Grey spheres are H atoms. Red points represents bond critical points, and crosses are ring critical points. NBO charges are from HF/aug-cc-pVTZ wave functions. Wiberg bond indices are given in parentheses.

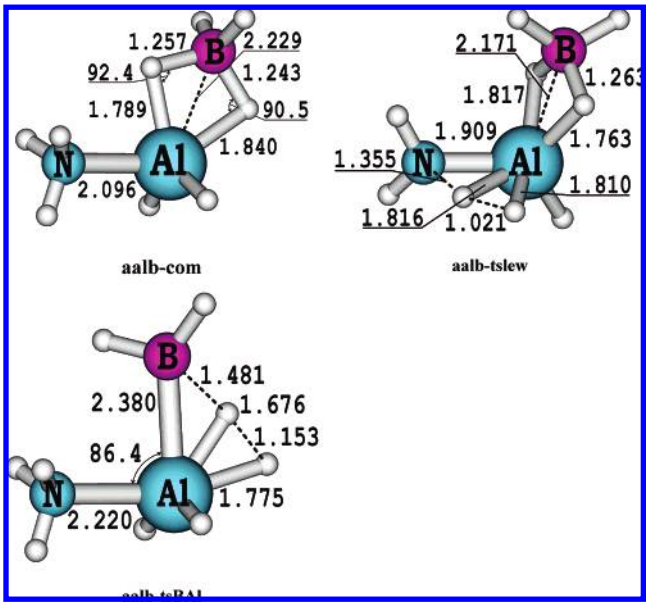

Figure 8. Selected MP2/aVTZ geometry parameters of an adduct **aalb-com** and the two transition states **aalb-tslew** and **aalb-tsBAl** related to the reaction $AlH_3NH_3 + BH_3$. Bond distances are in angstroms, and bond angles are in degrees.

double bridge is retained in **aalb-com** (Figure 8), whereas **abal-com** (Figure 5) contains a single Al−H−B bridge. A bridge bond is broken when ammonia approaches B rather than Al. The adduct **aalb-com** is stable relative to the reactants by 32.4 kcal/mol.

The two TS's located for the transformation of **aalb-com** (Figure 8) have many similarities with those from **aalal-com** (Figure 2). The **aalb-tsBAl** corresponding to a TS for H_2 release from AlH_3BH_3 is of high energy, 50.2 kcal/mol above the reactants **aal** + **b**. The **aalb-tslew** is a Lewis-type TS with a low energy, 3.3 kcal/mol below the reactants. Its high stability is due to the interaction of BH_3 with the TS **aal-ts** of the monomer via two B−H−Al bridge bonds. The product asymptote, $NH_2AlH_2BH_3 + H_2$, is only 1.6 kcal/mol above the adduct **aalb-com**. We were unable to locate a six-member cyclic TS similar to **abal-tsAlN**. Relative to the starting point **aal** + **b**, borane greatly facilitates release of H_2 from **aal**, but once the stable adduct **aalb-com** is formed, the process becomes more difficult, requiring 29.1 kcal/mol to reach **aalb-tslew**. Thus, there is no real catalytic effect due to borane for H_2 release from ammonia alane.

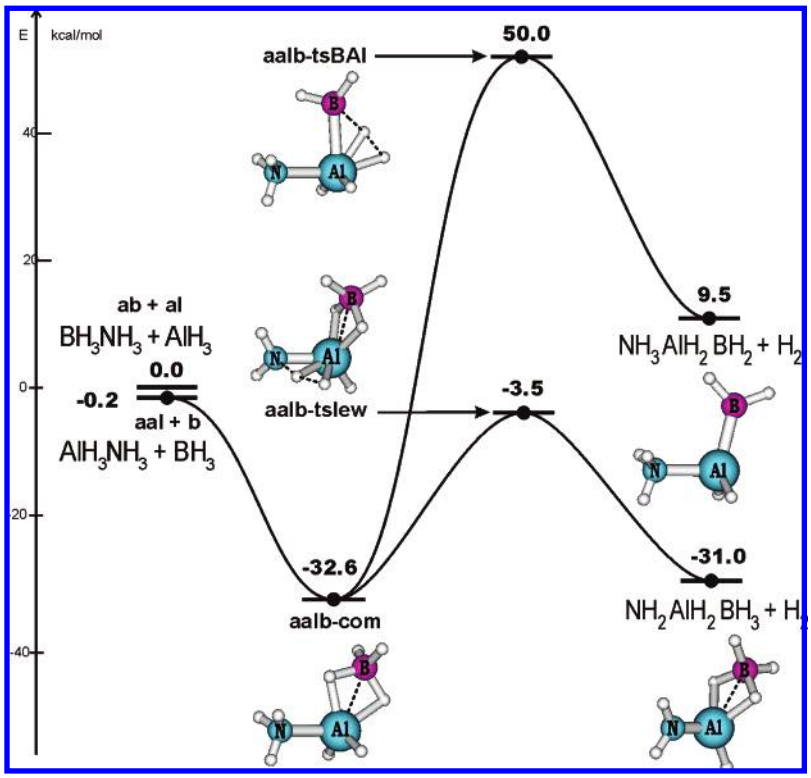

Figure 9. Schematic minimum-energy pathways for H_2 release from **aalb-com**. Relative energies in kcal/mol are from CCSD(T)/aVTZ + ZPE calculations.

TABLE 3: Relative Energy (kcal/mol) of the Reactants, Complexes, Transition States, and Products in the Processes of H_2 Elimination from AlH_3NH_3, AlH_3BH_3, and BH_3NH_3 in the Presence of AlH_3, BH_3, and NH_3

molecule	MP2/aVTZ[a]	CCSD(T)/aVDZ[b]	CCSD(T)/aVTZ[b]
$BH_3NH_3 + AlH_3$	0.0	0.0	0.0
$AlH_3NH_3 + BH_3$	0.4	0.5	−0.2
$AlH_3BH_3 + NH_3$	−12.3	−10.2	−12.0
$BH_2AlH_2NH_3 + H_2$	11.2	11.4	9.5
$BH_2NH_2 + AlH_3 + H_2$	−6.7	−5.6	−6.4
$NH_2BH_2AlH_3 + H_2$	−16.2	−11.7	−15.0
$NH_2AlH_2BH_3 + H_2$	−33.0	−24.1	−31.0
cyclic-$NH_2BH_2HAlH_2 + H_2$	−37.5	−31.3	−36.0
aalb-com	−33.1	−29.3	−32.6
abal-com	−17.9	−16.6	−18.9
abal-ts	18.3	18.9	17.8
aalb-tsBAl	52.3	51.6	50.0
abal-tsAlB	42.6	44.5	43.9
abal-tslewB	26.5	29.2	27.6
abal-tslewN	23.7	27.4	25.3
abal-tsAlN	−0.9	4.4	1.7
aalb-tslew	−5.4	2.2	−3.5

[a] MP2/aVTZ-optimized geometries. [b] Relative energies including zero-point contributions. Zero-point energies were obtained from MP2/aVDZ harmonic vibrational frequencies and scaled by a uniform scaling factor of 0.97.

Kinetics for Hydrogen Release Main Reactions. The lowest-energy reaction paths found in this work are

$$\textbf{aal} \rightarrow \textbf{a} + \textbf{al} \quad (9)$$

$$\textbf{aal} \rightarrow \textbf{aal-ts} \rightarrow AlH_2NH_2 + H_2 \quad (10)$$

$$\textbf{aalal-com} \rightarrow \textbf{aalal-tsAlN} \rightarrow NH_2AlH_2AlH_3 + H_2 \quad (11)$$

$$\textbf{abal-com} \rightarrow \textbf{abal-tsAlN} \rightarrow NH_2BH_2AlH_3 + H_2 \quad (12)$$

Table 4 lists the calculated rate constants, including tunneling corrections, using TST and RRKM theory for these processes. Table S4 shows the tunneling corrections at different temperatures for reactions 10−12.

Reaction 9 is barrierless and was treated just with the endothermicity for breaking the Al−N bond, and no tunneling corrections were calculated for this process. The TST rate constants are $k_\infty(298\ K) = 5.0 \times 10^{-5}\ s^{-1}$ and $k_\infty(400\ K) = 8.2\ s^{-1}$. The RRKM rate constants are predicted to be faster than those from TST by a factor of 2−4; $k(298\ K) = 2.2 \times 10^{-4}\ s^{-1}$ and $k(400\ K) = 17.0\ s^{-1}$.

For hydrogen elimination from the ammonia−alane complex (reaction 10), the TST rate constants (including tunneling corrections,[32] as described above) are $k_\infty(298\ K) = 1.95 \times 10^{-6}\ s^{-1}$ and $k_\infty(400\ K) = 8.92 \times 10^{-3}\ s^{-1}$. These are slower than the rate constant for dissociation of the Al−N bond in **aal**; therefore, AlH_3 will be produced rather than H_2, especially at temperatures around 125 °C.

TABLE 4: Rate Constants $k(T)$ Obtained by TST and RRKM Theory (in s^{-1}) at Different Temperatures (in Kelvin) Including Skodje and Truhlar Tunneling Corrections (Q_{ST})[a]

reaction	T	$Q_{ST}(T)$	TST	RRKM
aal → **a** + **al**[b]			$k_\infty(T) = 5.012 \times 10^{21}\, T^{-1.85}$ $\exp(-29.1/RT)$ s^{-1}	$k(T,p) = 8.128 \times 10^{9}\, p^{0.913}$ $\exp(-22.7/RT)$ s^{-1}
	298.15	–	5.02×10^{-5}	2.25×10^{-4}
	400	–	8.19	1.70×10^{1}
aal → **aal-ts** → $AlH_2NH_2 + H_2$			$k_\infty(T) = 1.995 \times 10^{11}\, T^{0.585}$ $\exp(-28.4/RT)$ s^{-1}	$k(T,p) = 3.981 \times 10^{10}\, p^{0.477}$ $\exp(-27.5/RT)$ s^{-1}
	298.15	2.29×10^{2}	1.95×10^{-6}	2.28×10^{-6}
	400	4.21	8.92×10^{-3}	1.01×10^{-2}
aalal-com → **aalal-tsAlN** → $NH_2AlH_2AlH_3 + H_2$			$k_\infty(T) = 1.995 \times 10^{10}\, T^{0.641}$ $\exp(-18.5/RT)$ s^{-1}	$k(T,p) = 7.943 \times 10^{9}\, p^{0.501}$ $\exp(-17.9/RT)$ s^{-1}
	298.15	1.13	2.58×10^{-2}	2.60×10^{-2}
	400	1.07	8.38×10^{1}	8.40×10^{1}
abal-com → **abal-tsAlN** → $NH_2BH_2AlH_3 + H_2$			$k_\infty(T) = 7.943 \times 10^{10}\, T^{0.284}$ $\exp(-19.4/RT)$ s^{-1}	$k(T,p) = 5.754 \times 10^{9}\, p^{0.45}$ $\exp(-18.9/RT)$ s^{-1}
	298.15	1.69	3.72×10^{-3}	4.36×10^{-3}
	400	1.32	1.36×10^{1}	1.54×10^{1}

[a] RRKM results are at 1 atm of p. The rate constants at 298.15 and 400 K include the tunneling correction. [b] Barrierless reaction.

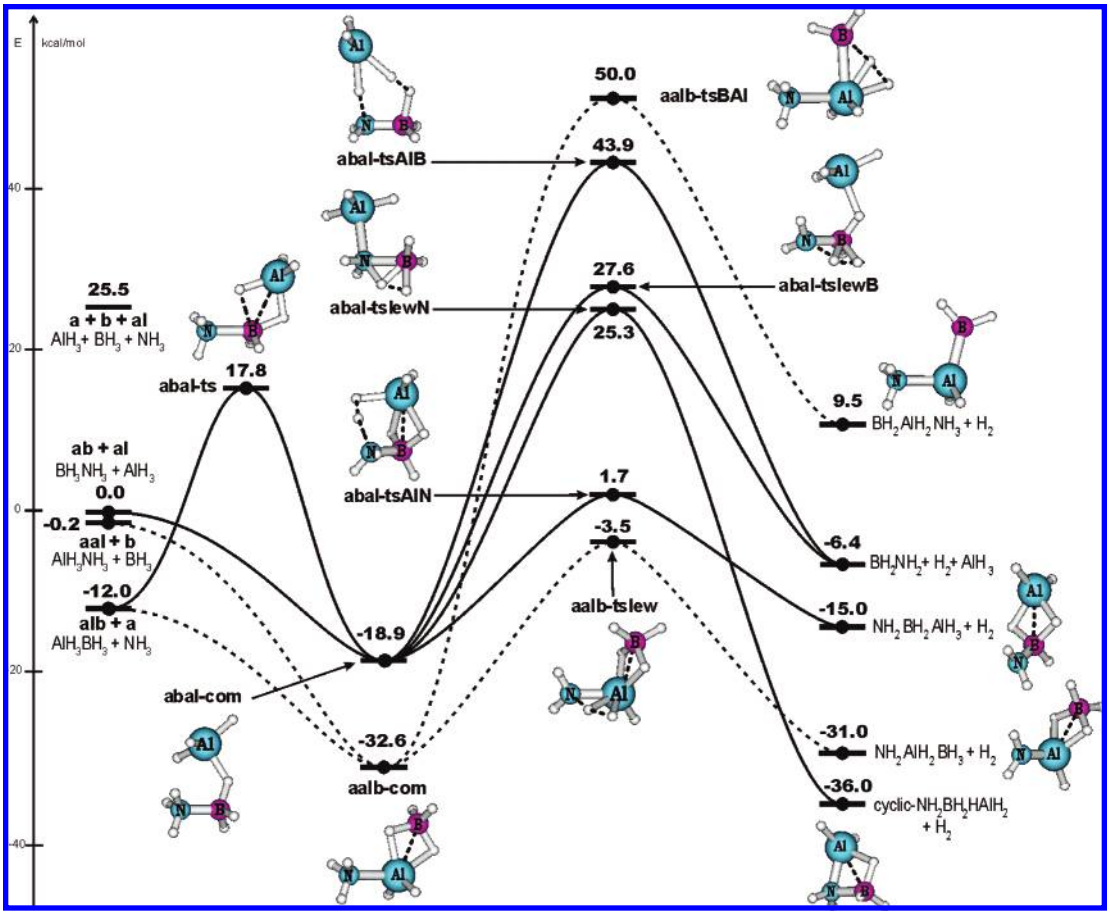

Figure 10. Overview of the potential energy surface of the molecular system $AlH_3 + BH_3 + NH_3$. Relative energies in kcal/mol are from CCSD(T)/aVTZ + ZPE calculations.

The decomposition of **aal** will produce alane, which can be a catalyst (reaction 11) for H_2 elimination. We predict corrected rate constants of $k_\infty(298\ K) = 2.58 \times 10^{-2}\ s^{-1}$ and $k_\infty(400\ K) = 8.38 \times 10^{1}\ s^{-1}$. For H_2 elimination from ammonia−borane with alane as the catalyst (eq 12), TST predicts $k_\infty(298\ K) = 3.72 \times 10^{-3}\ s^{-1}$ and $k_\infty(400\ K) = 1.54 \times 10^{1}\ s^{-1}$, including tunneling corrections. Similar results can be found with RRKM theory (see Table 4). Comparison of reactions 10 and 11 shows that reaction 11 is faster than reaction 10 by about 10^4 at 298 K, and this difference is reduced at 400 K. Reaction 11 is predicted to have a faster rate constant than that for reaction 13,[4] which has BH_3 as the catalyst for H_2 elimination from BH_3-NH_3

$$BH_3NH_3\cdots BH_3\ (\text{complex}) \rightarrow BH_2NH_2 + H_2 + BH_3 \qquad (13)$$

with $k_\infty(298\ K) = 6.1 \times 10^{-5}\ s^{-1}$ and $k_\infty(400\ K) = 1.06\ s^{-1}$, including tunneling.

The high-pressure limit for H_2 elimination is already reached at 1 atm, as the RRKM results for the rate constants are the same, or almost the same, at 1 and 11 atm. 3-D plots of the rate coefficients, k, as a function of temperature, T, and pressure,

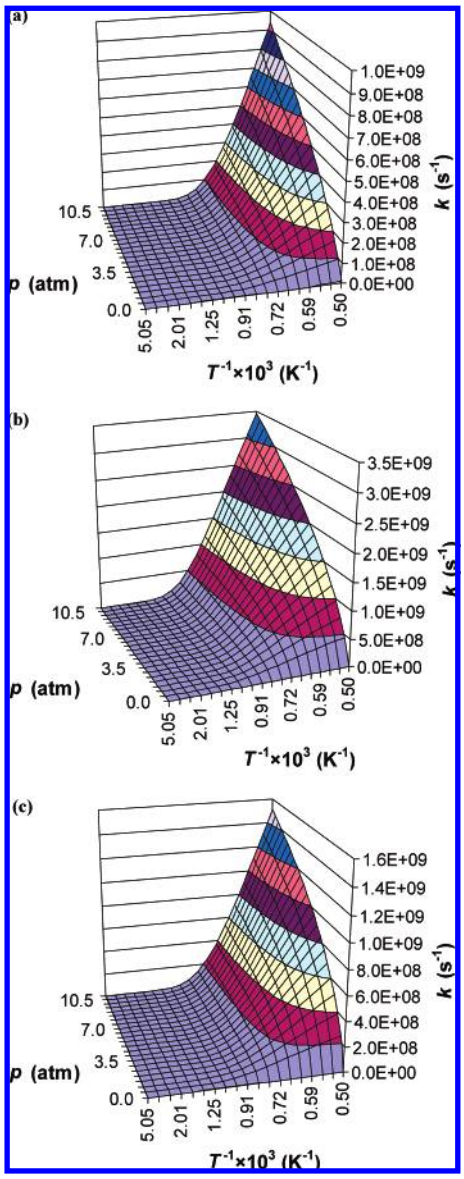

Figure 11. 3-D plots of the rate coefficients k using the RRKM method with N_2 as the bath gas in the temperature range (T) from 200 to 2000 K and pressure range (p) from 0.1 to 8360 Torr. Tunneling corrections are not included. (a) **aal** → **aal-ts** → $AlH_2NH_2 + H_2$; (b) **aalal-com** → **aalal-tsAlN** → $NH_2AlH_2AlH_3 + H_2$; and (c) **abal-com** → **abal-tsAlN** → $NH_2BH_2AlH_3 + H_2$.

p, using the RRKM method are shown in Figure 11. The tunneling corrections were not included in these plots.

Conclusion

In the present theoretical study, electronic structure calculations at the coupled-cluster theory CCSD(T) level in conjunction with the aug-cc-pVTZ basis set were employed to construct portions of the potential energy surfaces enclosing numerous minimum-energy pathways for H_2 release from ammonia alane (AlH_3NH_3) without and with the presence of alane (AlH_3). For the AlH_3NH_3 monomer, the energy barrier for hydrogen elimination is about 29 kcal/mol, and Al−N bond cleavage is about 2 kcal/mol energetically lower; therefore, the molecule will more likely dissociate into AlH_3 and NH_3 than lose H_2.

Figure 10 provides an overview of the various portions of the potential energy surface described above for the molecular system including ammonia, borane, and alane. Figure 10 is a superposition of the individual PES's with the same energy scale. The reactant asymptote $BH_3NH_3 + AlH_3$ is defined as the zero of energy. Relative energies are given in Table 3. Of the three possible starting reactants, $AlH_3BH_3 + NH_3$ is the most stable due to the high stability of AlH_3BH_3. The dissociation energy of AlH_3BH_3 giving AlH_3 and BH_3 is 38.4 kcal/mol, essentially the same as that of diborane to give two BH_3 molecules.[34] The $BH_3NH_3 + AlH_3$ and $AlH_3NH_3 + BH_3$ reactant asymptotes are essentially the same, ∼13 kcal/mol above $AlH_3BH_3 + NH_3$. The following pathway, **ab** + **al** (0.0 kcal/mol) → **abal-com** (−18.9) → **abal-tsAlN** (1.7) → $BH_2NH_2AlH_3 + H_2$ (−15.0) → $BH_2NH_2 + AlH_3 + H_2$ (−6.4), is the lowest-energy channel. The energy of the entire process ranges occurs within ∼20 kcal/mol. The transition state is only ∼2 kcal/mol above the starting reactants. The reaction is exothermic by ∼−6 kcal/mol starting from reactants, but the ultimate products with the catalyst regenerated are ∼12 kcal/mol above the adduct.

The reaction starting from the $AlH_3NH_3 + AlH_3$ asymptote (Figure 3) has the following lowest-energy pathway: **aal** + **al** (0.0 kcal/mol) → **aalal-com** (−23.0) → **aalal-tsAlN** (−4.3) → $NH_2AlH_2AlH_3 + H_2$ (−23.3) → $AlH_2NH_2 + AlH_3 + H_2$ (2.7). The overall reaction is marginally endothermic by ∼3 kcal/mol. The transition state is 4.3 kcal/mol below reactants and is 18.7 kcal/mol above the adduct. The adducts of both reactants and products are of similar energy, with an energy difference of ∼0.3 kcal/mol. The kinetic predictions show that AlH_3 can be produced by dissociation of the Al−N bond in AlH_3NH_3. The alane can then serve as an efficient bifunctional catalyst for H_2 release from ammonia alane. In addition, AlH_3 is a better catalyst for elimination of H_2 from BH_3NH_3 than is BH_3.

Acknowledgment. Funding was provided, in part, by the Department of Energy, Office of Energy Efficiency and Renewable Energy under the Hydrogen Storage Grand Challenge, Solicitation No. DE-PS36-03GO93013. This work was done as part of the Chemical Hydrogen Storage Center. David A. Dixon is indebted to the Robert Ramsay Endowment of the University of Alabama. M.T.N. is grateful to the FWO-Vlaanderen for supporting his sabbatical leave at the University of Alabama. V.S.N. thanks the Belgian Technical Cooperation Agency (BTC) for a scholarship.

Supporting Information Available: Optimized geometries (Cartesian coordinates and figures with selected parameters), CCSD(T) total energies, zero-point energies, and tunneling corrections. Figures S1 and S2 show the selected MP2/aug-cc-pVTZ geometry parameters for complexes and products for H_2 release from AlH_3NH_3, AlH_3BH_3, and BH_3NH_3 in the presence of AlH_3, BH_3, and NH_3 and H_2 loss from ethane catalyzed by AlH_3. This material is available free of charge via the Internet at http://pubs.acs.org.

References and Notes

(1) (a) Dressalhaus, M.; Crabtree, G.; Buchanan, M. *Basic Energy Needs for the Hydrogen Economy*: Basic Energy Sciences, Office of Science, U.S. Department of Energy: Washington, D.C., 2003. (b) Ramage, M. P. *The Hydrogen Economy: Opportunities, Costs, Barriers, and R&D Needs*; The National Academies Press: Washington, D. C., 2004.

(2) Stephens, F. H.; Pons, V.; Baker, R. T. *Dalton Trans.* **2007**, 2613.

(3) Dixon, D. A.; Gutowski, M. *J. Phys. Chem. A* **2005**, *109*, 5129.

(4) Nguyen, M. T.; Nguyen, V. S.; Matus, M. H.; Gopakumar, G.; Dixon, D. A. *J. Phys. Chem. A* **2007**, *111*, 679.

(5) (a) Stephens, F. H.; Baker, R. T.; Matus, M. H.; Grant, D. J.; Dixon, D. A. *Angew. Chem.* **2007**, *119*, 649. (b) Stephens, F. H.; Baker, R. T.; Matus, M. H.; Grant, D. J.; Dixon, D. A. *Angew. Chem., Int. Ed.* **2007**, *46*, 641.

(6) (a) Keaton, R. J.; Blacquiere, J. M.; Baker, R. T. *J. Am. Chem. Soc.* **2007**, *129*, 1844. (b) Chen, Y.; Fulton, J. L.; Linehan, J. L; Autrey, T. *J. Am. Chem. Soc.* **2005**, *127*, 3254. (c) Clark, T. J.; Russell, C. A.; Manners, I. *J. Am. Chem. Soc.* **2006**, *128*, 9582. (d) Denney, M. C.; Pons, V.; Hebden, T. J.; Heinekey, D. M.; Goldberg, K. J. *J. Am. Chem. Soc.* **2006**, *128*, 20481.

(7) Bluhm, M. E.; Bradley, M. G.; Butterick, R.; Kusari, U.; Sneddon, L. G. *J. Am. Chem. Soc.* **2006**, *128*, 7748.

(8) Matus, M. H.; Nguyen, M. T.; Dixon, D. A. *J. Phys. Chem. A* **2007**, *111*, 1726.

(9) Nguyen V. S.; Matus, M. H; Grant, D. J.; Nguyen, M. T.; Dixon, D. A. *J. Phys. Chem. A* **2007**, *111*, 8844.

(10) Stowe, A. C.; Shaw, W. J.; Linehan, J. C.; Schmid, B.; Autrey, T. *Phys. Chem. Chem. Phys.* **2007**, *9*, 1831.

(11) Nguyen, M. T.; Matus, M. H.; Dixon, D. A. *Inorg. Chem.* **2007**, *46*, 7561.

(12) Nguyen, V. S.; Matus, M. H; Nguyen, M. T.; Dixon, D. A. *J. Phys. Chem. C* **2007**, *111*, 9603.

(13) Yoon, C. W.; Sneddon, L. G. *J. Am. Chem. Soc.* **2006**, *128*, 13992.

(14) (a) Wang, P.; Kang, X. D.; Cheng, H. N. *ChemPhysChem* **2005**, *6*, 2488. (b) Balde, C. P.; Hereijgers, B. P. C.; Bitter, J. H.; de Jong, K. P. *Angew. Chem., Int. Ed.* **2006**, *45*, 3501. (c) Scholz, G.; Stosser, R.; Momand, J. A.; Zelh, A.; Klein, *Angew. Chem., Int. Ed.* **2000**, *39*, 2516.

(15) Yartys, V. A.; Denys, R. V.; Maehlan, J. P.; Frommen, C.; Fitcher, M.; Bulychev, M.; Emerich, H. *Inorg. Chem.* **2007**, *46*, 1051.

(16) Dou, D.; Ketchum, D. R.; Hamilton, E. J. M.; Florian, P. A.; Vermillion, K. E.; Grandinetti, P. J.; Shore, S. G. *Chem. Mater.* **1996**, *8*, 2839.

(17) Ashby, E. C. *J. Am. Chem. Soc.*, **1964**, *86*, 1882.

(18) Graetz, J.; Reilly, J. J.; Wegryzn, J. E. *Prepr. Pap. Am. Chem. Soc., Div. Fuel Chem.* **2007**, *52*, 447.

(19) (a) Grant, D. J.; Dixon, D. A. *J. Phys. Chem. A* **2005**, *109*, 10138. (b) Grant, D. J.; Dixon, D. A. *J. Phys. Chem. A* **2006**, *110*, 12955.

(20) Frisch, M. J.; Trucks, G. W.; Schlegel, H. B.; Scuseria, G. E.; Robb, M. A.; Cheeseman, J. R.; Montgomery, J. A., Jr.; Vreven, T.; Kudin, K. N.; Burant, J. C.; Millam, J. M.; Iyengar, S. S.; Tomasi, J.; Barone, V.; Mennucci, B.; Cossi, M.; Scalmani, G.; Rega, N.; Petersson, G. A.; Nakatsuji, H.; Hada, M.; Ehara, M.; Toyota, K.; Fukuda, R.; Hasegawa, J.; Ishida, M.; Nakajima, T.; Honda, Y.; Kitao, O.; Nakai, H.; Klene, M.; Li, X.; Knox, J. E.; Hratchian, H. P.; Cross, J. B.; Bakken, V.; Adamo, C.; Jaramillo, J.; Gomperts, R.; Stratmann, R. E.; Yazyev, O.; Austin, A. J.; Cammi, R.; Pomelli, C.; Ochterski, J. W.; Ayala, P. Y.; Morokuma, K.; Voth, G. A.; Salvador, P.; Dannenberg, J. J.; Zakrzewski, V. G.; Dapprich, S.; Daniels, A. D.; Strain, M. C.; Farkas, O.; Malick, D. K.; Rabuck, A. D.; Raghavachari, K.; Foresman, J. B.; Ortiz, J. V.; Cui, Q.; Baboul, A. G.; Clifford, S.; Cioslowski, J.; Stefanov, B. B.; Liu, G.; Liashenko, A.; Piskorz, P.; Komaromi, I.; Martin, R. L.; Fox, D. J.; Keith, T.; Al-Laham, M. A.; Peng, C. Y.; Nanayakkara, A.; Challacombe, M.; Gill, P. M. W.; Johnson, B.; Chen, W.; Wong, M. W.; Gonzalez, C.; Pople, J. A. *Gaussian 03*, revision C.01; Gaussian, Inc.: Wallingford, CT, 2004.

(21) Amos, R. D.; Bernhardsson, A.; Berning, A.; Celani, P.; Cooper, D. L.; Deegan, M. J. O.; Dobbyn, A. J.; Eckert, F.; Hampel, C.; Hetzer, G.; Knowles, P. J.; Korona, T.; Lindh, R.; Lloyd, A. W.; McNicholas, S. J.; Manby, F. R.; Meyer, W.; Mura, M. E.; Nicklass, A.; Palmieri, P.; Pitzer, R.; Rauhut, G., Schütz, M.; Schumann, U.; Stoll, H., Stone, A. J.; Tarroni, R.; Thorsteinsson, T.; Werner, H.-J. *MOLPRO*, a package of ab initio programs, version 2002.6; see http://molpro.net

(22) (a) Dunning, T. H., Jr. *J. Chem. Phys.* **1989**, *90*, 1007. (b) Kendall, R. A.; Dunning, T. H., Jr.; Harrison, R. J. *J. Chem. Phys.* **1992**, *96*, 6796.

(23) Pople, J. A.; Binkley, J. S.; Seeger, R. *Int. J. Quantum Chem., Quantum Chem. Symp.* **1976**, *10*, 1.

(24) (a) Purvis, G. D., III; Bartlett, R. J. *J. Chem. Phys.* **1982**, *76*, 1910. (b) Watt, J. D.; Gauss, J.; Bartlett. R. J. *J. Chem. Phys.* **1993**, *98*, 8718.

(25) Raghavachari, K.; Trucks, G. W.; Pople, J. A.; Head-Gordon, M. *Chem. Phys. Lett.* **1989**, *157*, 479.

(26) Dunning, T. H., Jr.; Peterson, K. A.; Wilson, A. K. *J. Chem. Phys.* **2001**, *114*, 9244.

(27) Peterson, K. A.; Woon, D. E.; Dunning, T. H., Jr. *J. Chem. Phys.* **1994**, *100*, 7410.

(28) Steinfeld, J. I.; Francisco, J. S.; Hase, W. L. *Chemical Kinetics and Dynamics*, 2nd ed.; Prentice Hall: New Jersey, 1999.

(29) (a) Kreevoy, M. M.; Truhlar, D. G. Transition State Theory. In *Investigations of Rates and Mechanisms of Reactions*, 4th ed., Bernasconi, C. F., Ed.; Wiley: New York, 1986. (b) Johnston, H. S. *Gas Phase Reaction Rate Theory*; Ronald Press: New York, 1966. (c) Glasstone, S.; Laidler, K. J.; Eyring, H. *The Theory of Rate Processes*; McGraw-Hill: New York, 1941. (d) Garrett, B. C.; Truhlar, D. G. Transition State Theory. In *Encyclopedia of Computational Chemistry*; Schleyer, P. v. R., Allinger, N. L., Clark, T., Gasteiger, J., Kollman, P. A., Schaefer, H. F., III, Eds.; John Wiley & Sons: Chichester, U.K., 1998.

(30) *(30) KHIMERA*, version 3.2: A software tool for calculations of chemical reactions thermodynamics and kinetics from first principles; Kintech, Kinetic Technologies, Ltd.: Moscow, 2003; see http://www.kintech.ru/.

(31) Holbrook, K. A.; Pilling, M. J.; Robertson, S. H. *Unimolecular Reactions*, 2nd ed.; Wiley: Chichester U.K., 1996.

(32) Skodje, R. T.; Truhlar, D. J. *J. Chem. Phys.* **1981**, *85*, 624.

(33) (a) Bader, R. F. W. *Atoms in Molecules, A Quantum Theory*; Oxford University Press: Oxford, U.K., 1995. (b) Popelier, P. *Atoms in Molecules, An Introduction*; Prentice Hall: Englewood Cliffs, NJ, 2000.

(34) Feller, D.; Dixon, D. A.; Peterson, K. A. *J. Phys. Chem. A* **1998**, *102*, 7053.